

# PROTECTION OF SENSITIVE INFILL IN FRAME BUILDINGS USING SB-UPGRADED ISOLATION SYSTEM: SEISMIC TESTS OF MODEL

Ilir Canaj<sup>(1)</sup>, Jelena Ristic<sup>(2)</sup>, Elena Dumova-Jovanoska<sup>(3)</sup>, Danilo Ristic<sup>(4)</sup>

<sup>(1)</sup> PhD student, Faculty of Civil Engineering, Ss. Cyril and Methodius University, Skopje, Republic of North Macedonia, e-mail: [ilirshcanaj@gmail.com](mailto:ilirshcanaj@gmail.com)

<sup>(2)</sup> Assoc. Prof. Dr. Sc., Faculty of Engineering, Department of Civil Engineering, International Balkan University (IBU), Skopje, Republic of North Macedonia, e-mail: [risticjelenaibu@gmail.com](mailto:risticjelenaibu@gmail.com)

<sup>(3)</sup> Prof. Dr. Sc., Faculty of Civil Engineering, Ss. Cyril and Methodius University, Skopje, Republic of North Macedonia, e-mail: [dumova@gf.ukim.edu.m](mailto:dumova@gf.ukim.edu.m)

<sup>(4)</sup> Prof. Dr. Sc., Institute of Earthquake Engineering and Engineering Seismology (IZIIS), Ss. Cyril and Methodius University, Skopje, Republic of North Macedonia, e-mail: [danilo.ristic@gmail.com](mailto:danilo.ristic@gmail.com)

## Abstract

This article presents an innovative construction system that provides efficient earthquake protection for sensitive infill panels in RC frame buildings. With qualitative upgrading of bulldog sliding base (SB) isolation system by incorporated novel uniform C-gaped energy dissipation devices, created was the new advanced sliding base C-gaped (SBC) system for seismic protection of buildings. Capability of the new seismic protection system of masonry infilled frame buildings was demonstrated with the conducted extensive seismic shaking table tests of large-scale model constructed with application of sliding base isolation system and created uniform C-gaped energy dissipation devices. The specific research segment devoted to development of the present SBC upgraded building system was originally initiated by the second and the fourth author and represent a part of the integral research project realized in the Institute of Earthquake Engineering and Engineering Seismology (IZIIS), Ss. Cyril and Methodius University in Skopje, during three and a half years research in the frames of the innovative NATO Science for Peace and Security Project “Seismic Upgrading of Bridges in South-East Europe by Innovative Technologies (SFP: 983828)”, involving five European countries. The composed upgraded isolated sliding system with uniform C-gaped energy dissipation (ED) devices represent suitably integrated passive mechanical building system providing harmonized response of integral buildings subjected to strong earthquakes. The adopted system is based on global optimization of seismic energy balance, achieved through utilization of newly designed energy dissipation devices as a supplementary damping to building isolation. The new SBC seismic protection system is based on incorporation of the following three integrated complementary systems: (1) Sliding base isolation system, (2) Created C-gaped energy dissipation (ED) system and (3) Displacement limiting (DL) system. The created SBC building system represents a qualitatively new construction strategy providing qualitatively upgraded seismic structural safety and efficient seismic protection of sensitive infill in rapidly constructed RC frame buildings located in seismically active regions.

*Keywords: frame building, masonry, framed masonry, seismic isolation, energy dissipation*

## 1. Introduction

The urgent need for seismic protection of frame buildings with sensitive infill is becoming clear from the recorded heavy damages of these structures during many earthquakes that have occurred worldwide (Japan, Turkey, South Europe, China, the USA, Italy, Taiwan, Chile, New Zealand, etc.). The initial studies in the field are documented in the published review of seismic base isolation research [1]. The renowned research centers worldwide have been performing continuous research toward reducing catastrophic earthquake consequences through improvement of regulations for design and construction of structures in seismically active regions, [2-6]. To increase the energy dissipation of the isolated system, specific U-shaped steel dampers have been studied and recommended for application, [7-9]. Earthquake damaging phenomena have been experimentally studied to define possible solution options, [10-12]. Many research projects have been initiated based on post-earthquake investigations of

earthquake consequences related to existing types of structures, [13-15]. Recently, extensive research involving shaking table tests on large-scale models have been conducted by the second and forth author and their collaborators, mainly targeted to seismic upgrading of isolated structures with specific energy dissipation devices, [16-18]. The basic design concept of reduced scale models for to be used for shaking table tests under simulated earthquakes, was adopted considering the data available from a completed similar research, [19]. The developed response modification method for seismic upgrading of new and existing building structures offers a very wide potential for practical application, particularly if refined nonlinear models and specific expert analysis procedures are consistently used, [20-23]. Presented in this paper is the developed innovative, multi-directional and uniform system applicable for advanced seismic protection of masonry and infilled frame masonry buildings. The new SBC building system was created based on adopted advanced upgrading of the initial sliding isolation system with the created new, efficient and experimentally proved C-gaped energy dissipation devices.

## 2. SBC Building System

Extensive experimental and analytical study was performed in the Institute of Earthquake Engineering and Engineering Seismology (IZIIS), Ss. Cyril and Methodius University (Skopje), as part of the NATO Science for Peace and Security Project “Seismic Upgrading of Bridges in South-East Europe by Innovative Technologies” (SFP: 983828), led by the fourth author. The developed SBC system represents a specific product of the extended part of the integrated research.

The new uniform building SBC-system has been developed based on the created compact passive C-gaped energy dissipation device providing uniform multi-directional response and qualitatively improved safety upgrading of buildings exposed to very strong earthquakes. The system has been formulated based on adopted concept of global optimization of the seismic energy balance. The designed C-gaped energy dissipation devices used as supplementary damping represent a qualitative system improvement in respect to the used building isolation only. The SBC system is based on incorporation of three complementary systems: (1) Basic seismic isolation system (SI system) providing low stiffness in horizontal direction; (2) The new C-gaped energy dissipation system to provide sufficient damping through dissipation of seismic energy, and, (3) Building displacement limiting (DL) devices to reduce or eliminate excessive displacements under strong impact effects. The intention was to create innovative SBC System with extended capability providing seismic protection of buildings exposed to strong near field and specific far field earthquakes, Figure 1.

## 3 C-gaped Devices

The new seismic energy dissipation system installed in the tested SBC building prototype model was composed of the developed advanced horizontal C multi-gap (HC-MG or C-gaped) energy dissipation (ED) devices. The original C-gaped energy dissipation devices of the proposed type, Fig.2, have been developed for bridges by the second author, [18]. The basic types of the created C-gaped ED components are presented in Table 1.

Table 1. Types of prototype models of C-Gaped (HC-MG) components

No.	Type	L1(mm)	do(mm)	d1(mm)	n
1	HC-1.1	L1 = 180 mm	do = 18.0 mm	d1 = 25.0 mm	25
2	HC-1.2	L1 = 180 mm	do = 12.0 mm	d1 = 18.5 mm	25
3	HC-1.3	L1 = 180 mm	do = 12.0 mm	d1 = 15.0 mm	25
4	HC-2.1	L2 = 150 mm	do = 18.0 mm	d1 = 25.0 mm	25
5	HC-2.2	L2 = 150 mm	do = 12.0 mm	d1 = 18.5 mm	25
6	HC-2.3	L2 = 150 mm	do = 12.0 mm	d1 = 15.0 mm	25

With conducted experimental testing under cyclic loading, Fig. 3, and with refined 3D nonlinear analytical modelling, the hysteretic responses of the created C-gapped energy dissipation components were defined. With the computed original results, it was confirmed that the adopted representative

gaped-bilinear analytical model could be implemented to realistically model the hysteretic behavior of the individual device components.

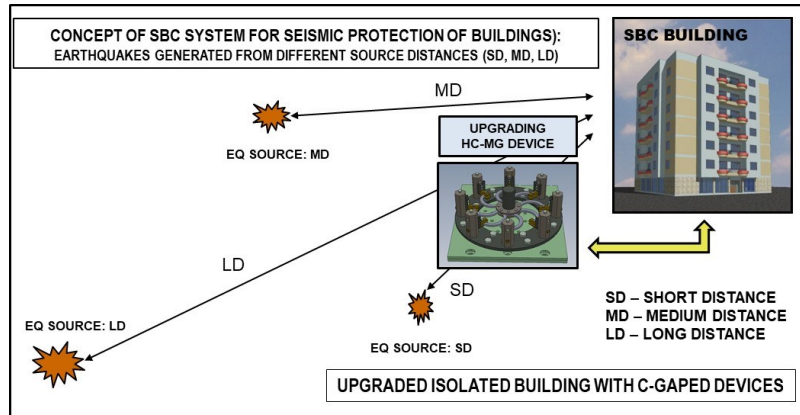


Figure 1. Concept of innovative SBC System for seismic protection of buildings

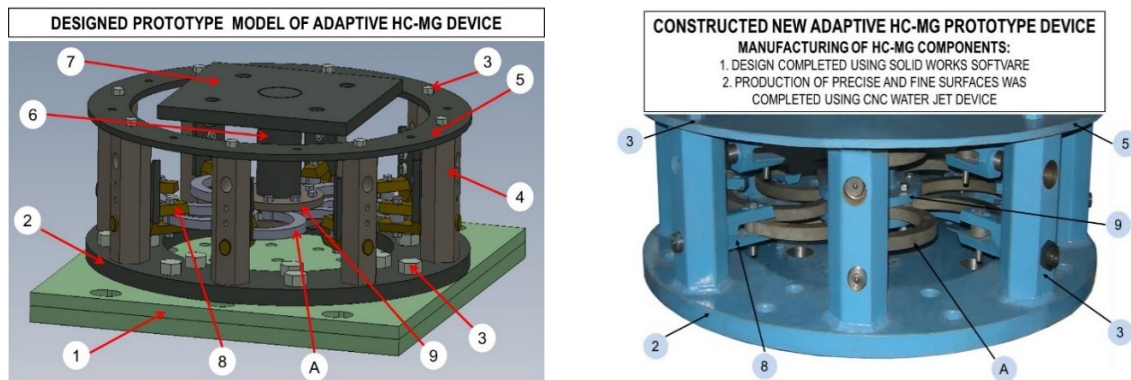


Figure 2. Designed and constructed prototype model of C-Gaped (HC-MG) device consisting of: 1. Bottom fixing plate; 2. Base ring plate; 3. Connecting bolts; 4. Vertical side supports; 5. Upper ring plate; 6. Central support; 7. Upper fixing plate; 8. Gap hinge device; 9. Central hinge device; A. HC-MG components at level L1. Figure right shows the prototype device with assembled HC-MG components of type HC-1.2 (at level L1 with gap G1 and at level L2 with gap G2), Originally developed for bridges [18].

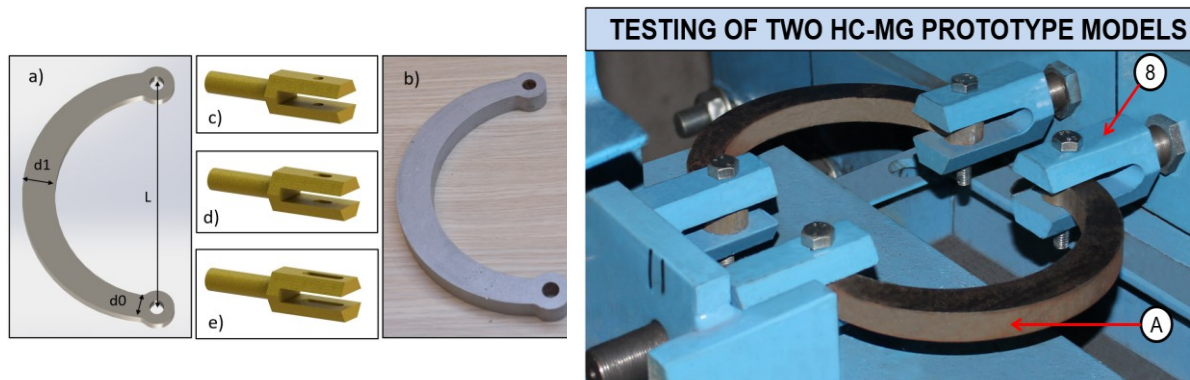


Figure 3. Constructed and tested gapped HC-MG energy dissipation components: prototypes of HC-MG components and supporting devices (left) and test setup for testing of two HC-MG prototype models (right)

## 4 Models of Isolation and Displacement Limiting Devices

### 4.1 Models of DSSSB isolation devices

The present isolation system used for the experimental SBC building model was assembled by use of the developed scaled models of double spherical sliding seismic bearing (DSSSB) devices with two large-radii of spherical surfaces, Fig. 4. The DSSSB devices were originally designed, constructed and used in a previous investigation carried out by Ristic, J., et al., 2023, [23]. The targets that were set prior to the design and construction of the device were fulfilled: (1) very small horizontal reaction and friction forces (reaching maximum 4.3% of the vertical load), and (2) stable hysteretic behavior along the entire range of large displacements. It was confirmed that the hysteretic behavior of the implemented DSSSB devices could be successfully simulated with the experimentally defined representative bilinear analytical model.

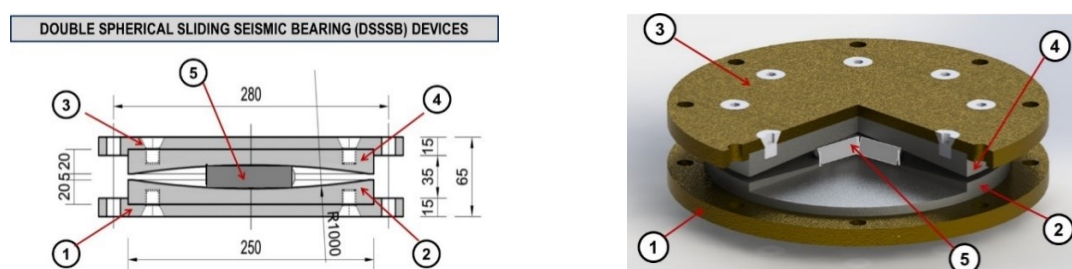


Figure 4. Components of the constructed and used prototypes of DSSSB devices: (1) lower end metal plate; (2) lower spherical plate; (3) upper end metal plate; (4) upper spherical plate; (5) metallic slider.

Actually, the model was controlled by four parameters,  $DY=1.0$  mm,  $FY=0.32$  kN,  $DU=50.0$  mm,  $FU=0.92$  kN, defined experimentally under simulated vertical load and cyclic displacements with increasing amplitudes.

### 4.2 Models of displacement limiting devices

The constructed and implemented DL system in the tested SBC model consisted of built-in four limiting devices marked by (6) in Fig. 7. The implemented DL devices were installed with a predefined gap. In practice, the new, specially designed and experimentally tested rubber buffers [18] can be an advanced solution.

## 5 Seismic Tests of SBC Building Model

### 5.1 Construction of SBC building model

The constructed model of the innovative SBC building prototype is shown in Fig. 5 and Fig. 6. The concept of the created model was specifically targeted on assuring conditions for realistic experimental simulation of pre-defined important testing objectives. The basic geometrical characteristics of the SBC building model, the available size of the seismic shaking table and the implemented instrumentation system of the SBC building model, were considered and harmonized accordingly. Regarding the shaking table dimensions, its loading capacity and related characteristics, a geometric scale factor,  $l_r$ , of 1:4 was adopted. In order to preserve the model similarity, all the other characteristics related to the dynamic tests needed to be properly scaled. Considering the important factors addressed, the combined true replica-artificial mass simulation model was adopted as the most adequate. The scale factors for different physical quantities were defined as a function of the geometrical scale factor, according to the similitude law, [18] and [19]. The building prototype model, Fig. 5, Fig. 6 and Fig. 7, was constructed with dimensions of  $a=314.0$  cm and  $b=174.0$  cm at plan, while the considered total model height was  $h=231.0$  cm. The frame system of the model consisted of RC columns (8) with section dimensions 12.0 cm x 12.0 cm, horizontal RC beams, in both directions, with section dimensions 12.0 cm x 12.0 cm and



two integrating monolithic RC slabs with thickness of 8.0 cm, spaced between the RC beams. The masonry walls (9) having characteristic door and window openings (10), were constructed using plain brick with a width of 9.0 cm. The model-base isolated monolithic RC slab (7) was constructed with thickness of 15.0 cm. The upper part of the building model (the superstructure part) rested on four DSSSB devices (4) placed on constructed four special steel spacers (3). At both ends, between the DSSSB isolators, the two new C-gaped devices (5) for energy dissipation were installed, Fig. 7.

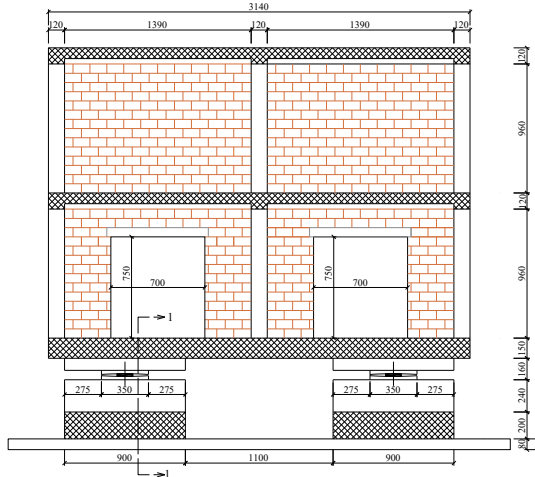


Figure 5. Side view of seismically tested SBC large-scale building scale prototype model.

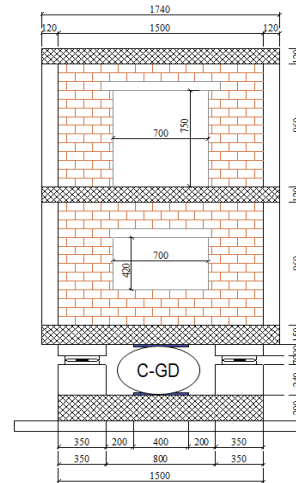


Figure 6. Front view of seismically tested SBC large-scale building scale prototype model.

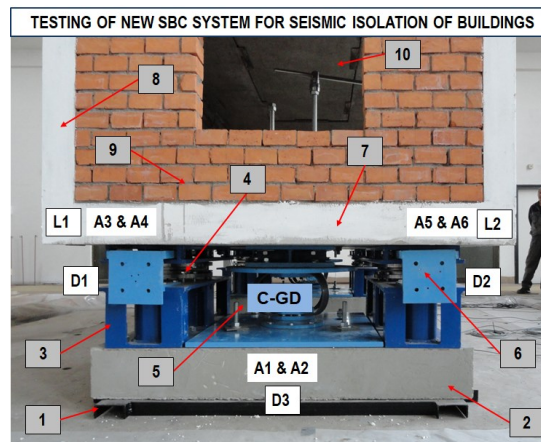


Figure 7. Isolation system of the SBC model: Installed four DSSSB devices (4), Installed two novel C-gaped energy dissipation devices (5) and the implemented four DL devices (6).

Similarly, at each model end, there were provided two DL devices in a cylindrical form that were tested before as special rubber buffers, (6). The integral SBC system was supported by two RC slabs (2), proportioned 90 x 150x 20 cm, connected to the integrating base-metal frame (1), fixed to the seismic shaking table. Eight metal elements with bulk density of 400 kg each were installed on the three RC model slabs to appropriately increase the total mass of the model. Their distribution per story was 2+2+4. The DL devices were installed at 50mm gaps to prevent the destructive effects of possible excessive displacements. All steel parts were manufactured to a reduced scale by use of S355 steel material, while concrete C25/30 was used for construction of all RC parts of the constructed model. The existing laboratory seismic shaking-table was square-shaped (5.0 by 5.0 m). Seismic input could be applied in one horizontal and in vertical direction. To adapt the large-scale SBC model for seismic testing, its longitudinal axis was positioned to coincide with the direction of motion of the shaking table,

Fig. 8. In that way, generation of seismic forces was enabled in longitudinal direction of the SBC model. The SBC test model was integrally assembled on the shaking table and equipped with the defined instrumentation system. For seismic testing of the SBC prototype model, the model superstructure (isolated building) rested on four DSSSB isolators spaced at the two model ends (using pairs of devices at each end), Fig. 7 and Fig. 8. The two C-gaped energy dissipation devices at both model ends were installed between the installed DSSSB seismic isolators, Fig. 7.

## 5.2. SBC building model instrumentation

To ensure acquisition of all the required data during the conducted dynamic tests, a well-designed instrumentation system was installed. The SBC large-scale prototype model assembled on the seismic shaking table was experimentally tested under compressed real strong earthquakes, according to the model scaling and similarity conditions. The selected strong earthquakes were simulated in the considered representative longitudinal direction of the constructed model. Actually, the designed instrumentation system of the model consisted of three different types of sensors, Fig. 7 and Fig. 8:

(a) *Transducers of the type of LVDT, representing displacement sensors*: Three displacement sensors were installed to measure relative displacements in longitudinal direction. The first two transducers of the type of LVDT, marked as D1 and D2, were used for recording time histories of relative displacements between the base-support of the isolation system and the bottom RC model slab located just above the seismic isolation devices. In addition, the third transducer of the type of LVDT, marked as D3, was used to measure possible relative displacements between the shaking table and the lowest fixed steel segment supporting the entire model structure;

(b) *Transducers of the type of LP, representing linear potentiometers*: Six sensors of the type of LP were used to measure the total displacements of the isolated building model in longitudinal direction. The first two transducers marked as L1 and L2 were located on the left and the right side of the bottom RC model slab, the next two transducers, L3 and L4, were installed on the left and the right side of the middle RC slab, and the last two transducers, L5 and L6, were spaced at respective locations on the top RC model slab. To assure conditions for such measurement, the second ends of the linear potentiometers were connected to the provided appropriate connection points. The required connection points were located in the constructed additional steel frame directly fixed to the existing, no excited, laboratory floor, spaced with a respective gap around the moving shaking table.

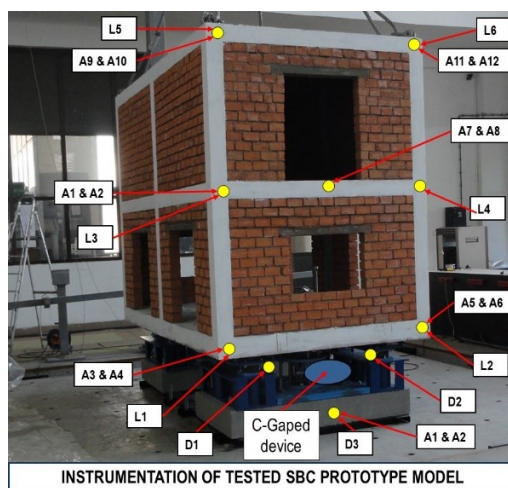


Figure 8. Used acquisition points and sensors for recording channels of SBC building model tested on seismic shaking table under simulated strong earthquakes.

(c) *Transducers of the type of ACC, representing acceleration sensors*: A total of twelve sensors of the type of ACC were installed, providing thus a pair of sensors at each of the selected six characteristic locations. The first and the second ACC sensor at each considered location were properly directed to measure acceleration time-histories in longitudinal (L) and transversal (T) direction, respectively. In the

first (the lowest) ACC location, there were provided two measuring channels (A1 & A2), recording accelerations in longitudinal (L) and transversal (T) direction, respectively. Following the same instrumentation concept, at each of the next five ACC locations, two measuring channels were similarly provided. The first and the second channel (Ai & Aj) at each location were similarly used for recording accelerations in longitudinal (L) and transversal (T) direction, respectively.

### 5.3 Seismic tests of SBC building model

**(a) SBC Model assembling:** The new SBC building prototype model, Fig. 8, was assembled, incorporating four DSSSB isolation devices, two C-gaped energy dissipation devices and four displacement limiting (DL) devices, Fig. 7. The created C-gaped energy dissipation devices were composed by installation of pre-defined four prototypes of energy dissipation components, Table. 1.

**(b) Tests with sine-sweep:** The dynamic tests carried out by simulated sine-sweep dynamic inputs, 0.02g and 0.04g, covering a range of frequencies from 1 to 35Hz and the use of the provided data sources, enabled definition of: (1) the initial fundamental period amounting to  $T_0=0.461$ s, corresponding to the case of the building model with installed DSSSB devices only. The new C-gaped devices were not connected and not activated; and (2) Damping between 3.0 and 3.4%.

**(c) Comparative testing:** To assess the contribution of the C-gaped devices to energy dissipation, the model was first tested with installed DSSSB isolators only, under simulated Petrovac earthquake scaled to  $PGA = 0.47$  g. The comparative relative displacements recorded under equal test conditions for the system composed with and without C-gaped devices are presented in Fig. 10. It was shown that the building model with installed C-gaped devices represented a highly favorable upgrading option. For the system with seismic isolation only, an unacceptable relative displacement amounting to  $D_e = 42.6$  mm was obtained. This excessive response actually represented the critical state, because the displacement limit of the used seismic isolators was 40.0 mm. However, regarding the SBC system with the new C-gaped devices, the relative displacement was reduced to a fully controlled value of  $D_c = 24.69$  mm, representing an important reduction of -38.2%.

#### **(d) Summary of testing conditions and selected results, including:**

**d1) Seismic input:** Seismic testing of the new SBC building model was carried out using four selected real earthquake records. Actually, to obtain representative experimental data, representative earthquake intensities were considered in all testing cases. The seismic input intensities were generated considering controlled high (possible) values of peak ground accelerations amounting to  $PGA=0.42g$  for the El Centro (1940) record,  $PGA=0.48g$  for the Petrovac (Montenegro, 1979) record,  $PGA=0.51g$  for the Landers record and  $PGA=0.29g$  for the Northridge record, respectively. Following the similitude law, the original earthquake records were time compressed for a time factor of  $1/2$ , as a square root of  $I_r$ .

Table 2. Maximum positive and negative relative displacements recorded by the installed LVDT sensors, during the conducted four original seismic tests of SBC prototype model

No.	O-T1: C-El-Centro, $PGA=0.42G$			O-T2: C-Petrovac, $PGA=0.48G$		
	Channel	MaxD (-) (mm)	MaxD (+) (mm)	Channel	MaxD (-) (mm)	MaxD (+) (mm)
1	LVDT-01	-30.27	24.60	LVDT-01	-21.90	21.62
2	LVDT-02	-36.34	24.38	LVDT-02	-24.69	21.69
3	LVDT-03	-8.79	6.49	LVDT-03	-6.37	6.61
No.	O-T1: C-Landers, $PGA=0.51G$			O-T2: C-Nortrige, $PGA=0.29G$		
	Channel	MaxD (-) (mm)	MaxD (+) (mm)	Channel	MaxD (-) (mm)	MaxD (+) (mm)
1	LVDT-01	-22.95	27.72	LVDT-01	-31.40	20.92
2	LVDT-02	-26.11	29.50	LVDT-02	-36.36	20.98
3	LVDT-03	-8.52	6.62	LVDT-03	-9.06	0.00

d2) *Data acquisition*: Extensive experimental data files were recorded from each acquisition channel. The integral data recording system included the full set of 21 channels instrumented with sensors according to the model instrumentation plan and additional extra sensors were used for full control of the shaking table. Having such an extensive instrumentation system and refined data sampling rate from each seismic test, about 5 million numerical values were recorded. The testing process consisting of nine seismic tests, was completed very successfully and all sensors provided correct and complete experimental records continuously. The representative results showing the actual system response were selected, presented and discussed.

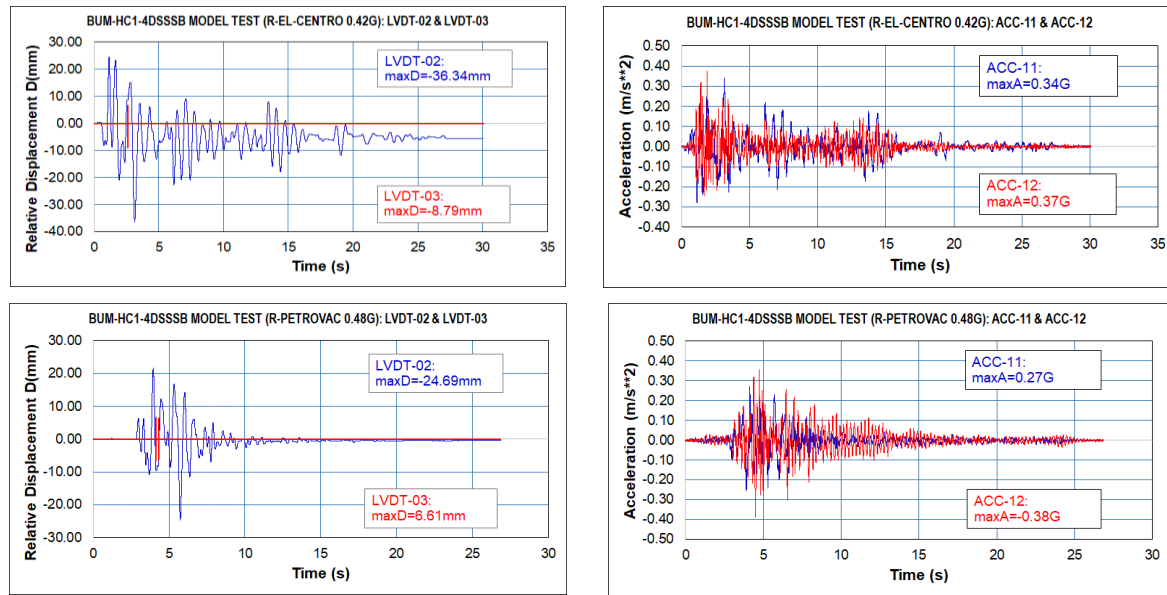


Figure 9. Relative displacements of the SBC model-base (left) and recorded acceleration responses by ACC-11 & ACC-12 (right) during the tests carried out under simulated El-Centro and Petrovac earthquake.

Table 3. Maximum positive and negative displacements recorded by the installed LP sensors during the conducted four original seismic tests of the new SBC prototype model

No.	O-T1: C-El-Centro, PGA=0.42G			O-T2: C-Petrovac, PGA=0.48G		
	Channel	MaxD (-) (mm)	MaxD (+) (mm)	Channel	MaxD (-) (mm)	MaxD (+) (mm)
1	LP-01	-47.49	-47.49	LP-01	-20.96	16.89
2	LP-02	-51.89	-51.89	LP-02	-22.22	15.96
3	LP-03	-48.80	-48.80	LP-03	-22.08	17.71
4	LP-04	-52.95	-52.95	LP-04	-23.19	16.59
5	LP-05	-49.64	-49.64	LP-05	-22.90	18.13
6	LP-06	-54.08	-54.08	LP-06	-23.93	16.90

No.	O-T1: C-Landers, PGA=0.51G			O-T2: C- Nortrige, PGA=0.29G		
	Channel	MaxD (-) (mm)	MaxD (+) (mm)	Channel	MaxD (-) (mm)	MaxD (+) (mm)
1	LP-01	-12.40	21.51	LP-01	-52.59	41.58
2	LP-02	-14.03	21.26	LP-02	-55.23	41.14
3	LP-03	-13.72	22.60	LP-03	-54.14	42.45
4	LP-04	-15.05	22.29	LP-04	-56.09	42.23
5	LP-05	-14.53	23.28	LP-05	-54.91	43.45
6	LP-06	-15.75	22.96	LP-06	-57.30	42.18



Table 4. Maximum positive and negative accelerations recorded by the installed ACC sensors during the conducted four original seismic tests of the new SBC prototype model

O-T1: C-El-Centro, PGA=0.42G						O-T2: C-Petrovac, PGA=0.48G				
No.	Channel	MaxA G (-)	DAF	MaxA G (+)	DAF	Channel	MaxA G (-)	DAF	MaxA G (+)	DAF
1	ACC-01	-0.40	0.95	0.43	1.02	ACC-01	-0.51	1.06	0.40	0.82
2	ACC-02	-0.09	0.21	0.10	0.23	ACC-02	-0.07	0.14	0.07	0.14
3	ACC-03	-0.30	0.71	0.31	0.73	ACC-03	-0.29	0.60	0.21	0.43
4	ACC-04	-0.22	0.52	0.24	0.57	ACC-04	-0.21	0.43	0.32	0.66
5	ACC-05	-0.23	0.54	0.31	0.73	ACC-05	-0.22	0.45	0.21	0.43
6	ACC-06	-0.22	0.52	0.24	0.57	ACC-06	-0.20	0.41	0.32	0.66
7	ACC-07	-0.21	0.50	0.24	0.57	ACC-07	-0.20	0.41	0.19	0.39
8	ACC-08	-0.23	0.54	0.19	0.45	ACC-08	-0.25	0.52	0.31	0.64
9	ACC-09	-0.32	0.76	0.34	0.80	ACC-09	-0.28	0.58	0.35	0.72
10	ACC-10	-0.29	0.69	0.38	0.90	ACC-10	-0.39	0.81	0.36	0.75
11	ACC-11	-0.27	0.64	0.34	0.80	ACC-11	-0.25	0.52	0.27	0.56
12	ACC-12	-0.28	0.66	0.37	0.88	ACC-12	-0.38	0.79	0.35	0.72

O-T1: C-Landers, PGA=0.51G						O-T2: C- Northridge, PGA=0.29G				
No.	Channel	MaxA G (-)	DAF	MaxA G (+)	DAF	Channel	MaxA G (-)	DAF	MaxA G (+)	DAF
1	ACC-01	-0.54	1.05	0.44	0.86	ACC-01	-0.20	0.68	0.31	1.06
2	ACC-02	-0.07	0.13	0.09	0.17	ACC-02	-0.05	0.17	0.05	0.17
3	ACC-03	-0.37	0.72	0.29	0.56	ACC-03	-0.22	0.75	0.28	0.96
4	ACC-04	-0.33	0.64	0.31	0.60	ACC-04	-0.16	0.55	0.19	0.65
5	ACC-05	-0.32	0.62	0.30	0.58	ACC-05	-0.23	0.79	0.29	1.00
6	ACC-06	-0.32	0.62	0.31	0.60	ACC-06	-0.16	0.55	0.19	0.65
7	ACC-07	-0.21	0.41	0.22	0.43	ACC-07	-0.20	0.68	0.25	0.86
8	ACC-08	-0.28	0.54	0.33	0.64	ACC-08	-0.15	0.51	0.14	0.48
9	ACC-09	-0.34	0.66	0.36	0.70	ACC-09	-0.23	0.79	0.30	1.03
10	ACC-10	-0.39	0.76	0.37	0.72	ACC-10	-0.11	0.37	0.23	0.79
11	ACC-11	-0.34	0.66	0.31	0.60	ACC-11	-0.22	0.75	0.29	1.00
12	ACC-12	-0.38	0.74	0.36	0.70	ACC-12	-0.11	0.37	0.23	0.79

(d3) *Relative displacements*: The relative peak displacements, including positive and negative pulses, recorded during the seismic tests of the SBC system under the simulated El-Centro, Petrovac, Landers and Northridge earthquake are presented in Table 2. Comparatively, Fig. 9 (left) shows the recorded time-histories of relative displacement responses in longitudinal (L) direction during the tests carried out by simulation of the El-Centro and Petrovac earthquake, respectively. Regarding the presented experimental results, the following important observations were made: (1) The recorded relative displacements in L direction (direction of earthquake excitation) were dominant; (2) It was confirmed that the test model was successfully fixed to the shaking table since the relative displacements in L direction recorded by LVDT-03 were very small in all test cases; (3) The absolute maximum recorded relative displacement amounting to  $D_{max} = 36.36$  mm was below the critical (allowable) relative displacement of the seismic isolators amounting to  $D_a = 40.0$  mm, and (4) Seismic response of the assembled SBC system that was tested repeatedly twice appeared to be very similar. The results from the conducted original series of tests-1 are presented (O-Ti) in Tables 2 to 4. Consequently, the series of repeated seismic tests-2 (not presented) were realized using the same four earthquakes. Only small, negligible differences of maximum displacements were observed.

(d4) *Accelerations*: The representative time-histories of accelerations recorded by sensors ACC-11 and ACC-12, respectively in L and T-direction, during the seismic tests on the SBC model conducted under the simulated El-Centro and Petrovac earthquakes are comparatively shown in Fig. 9 (right).

However, Table 4 shows the representative peak accelerations recorded by all sensors, namely, ACC-01 to ACC-12. At each measuring point, accelerations were recorded in L and in T-direction during the seismic tests on the SBC model conducted under the simulated all four representative earthquakes. Considering the presented results, it was confirmed that: (1) The recorded accelerations at the superstructure, respectively in L and T-direction, were quite small (without amplification); and (2) Due to the present regular fluctuation, the recorded accelerations at the superstructure in L and T-direction were with similar peak values and in the expected range; (3) The new SBC system showed sustainability since the response parameters recorded during the original (O) tests-1 and the repeated tests-2 were quite similar, and (4) Generally, the DAF (dynamic amplification factor) values presented in the same Table 4 were quite small (smaller than 1.0), demonstrating favorable and consistent response. It was confirmed that the obtained relations between the maximum response and the maximum input acceleration ( $DAF = A_r/PGA$ ) were within the expected ranges in all cases.

(d5) *Absolute displacements*: The absolute displacement responses (in L -direction) recorded by the six LP sensors, Table 3, installed on the SBC model, proved existence of small inter-story drifts and successful control of the shaking table in all realized testing cases.

(d6) *System advances*: Generally, the new SBC system exhibited safe and very favorable behavior under strong earthquake excitations. Considering the processing of more than 50.000.000 recorded original numerical values obtained from the realized fifteen shaking table tests, the main qualitative advances of the innovative SBC system upgraded with C-gaped energy dissipation devices, are summarized in Fig. 10. Stable, reliable and safe seismic response was observed in all test cases due to the provided significant reduction of maximum relative displacements amounting to 9.1%, 38.2%, 26.2% and 9.1%, respectively, in the case of the simulated El Centro, Petrovac, Landers and Northridge earthquakes. All recorded peak values were lower than the defined allowable design displacement of  $D_a=40.0\text{mm}$  for the seismic isolators. The importance of upgrading the isolated masonry and infilled frame buildings with the new C-gaped devices was experimentally validated and confirmed with the conducted initial quantification test of the model with the installed seismic isolation only. Under the simulated strong Petrovac earthquake, the tested system without C-gaped devices showed an unsafe response to the recorded excessive relative displacement amounting to  $\max D=42.6\text{ mm}$ , Fig. 10.

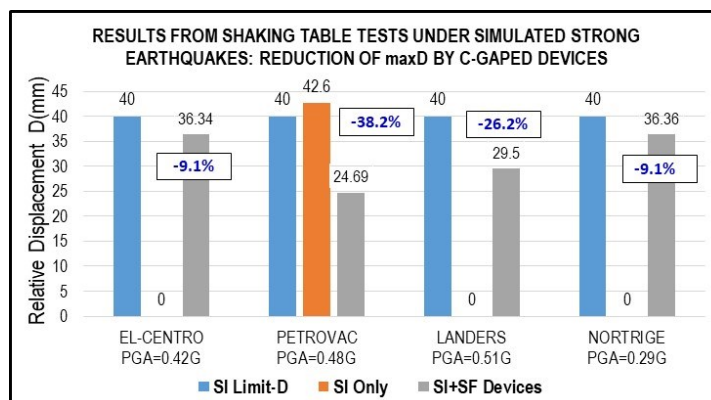


Figure 10. Advances of the SBC system: Reduction of maximum relative displacements defined from the conducted seismic tests under simulated strong earthquakes.

## 6 Conclusions

Considering the results obtained from the conducted experimental study, the following conclusions are derived: (1) The new SBC building system represents efficient and experimentally proved option for seismic protection of framed masonry buildings and their sensitive infill. The system provided significant modification of seismic response of the integral structure, resulting in efficient protection of buildings subjected to strong near field earthquakes; (2) The originally designed, constructed and implemented double spherical sliding bearing (DSSSB) devices [18], were confirmed as favorable types

of isolation bearings for the new SBC isolation system; (3) The created uniform C-gaped energy dissipation devices exhibited very good energy dissipation capacity. Their capability to exhibit stable hysteretic response under arbitrary earthquake excitation was clearly confirmed. In addition, the new C-gaped energy dissipation devices preserve their dissipation capability even in the cases of repeated strong earthquake loading; (4) The displacement limiting (DL) devices of the building should be considered as an obligatory constituent element of the created SBC system serving as the last defense line against excessive displacements of the integral building. Their appropriate design is an important step toward providing their activation only in the critical cases of very strong and abrupt earthquakes; (5) The three-dimensional, hysteretic, uniform and multi-directional response of the new C-gaped energy dissipation devices can be successfully predicted by application of the refined nonlinear micro-modeling with the adopted bilinear kinematic hardening steel material model; (6) The present study resulted in development of an experimentally proved design concept. The developed design concept can assure practical application of the new SBC system for seismic protection of framed masonry buildings located in seismic regions.

## Acknowledgements

The present study represents a supplemental part of the long-term innovative NATO Science for Peace and Security Project: Seismic Upgrading of Bridges in South-East Europe by Innovative Technologies (SFP: 983828). The extended NATO support to the realization of the extensive innovative research is highly appreciated.

## References

- [1] Kelly, J. M. (1986): Aseismic Base Isolation: A Review and Bibliography, *Soil Dynamics and Earthquake Engineering* 5, 202–216. [DOI]
- [2] Robinson, W. H. (1982): Lead-Rubber Hysteretic Bearings Suitable for Protecting Structures During Earthquakes, *Earthquake Engineering and Structural Dynamics* 10, 593–604. [DOI]
- [3] Iemura, H., Taghikhany, T., Jain, S. K. (2007): Optimum Design of Resilient Sliding Isolation System for Seismic Protection of Equipment, *Bulletin of Earthquake Engineering* 5, 85–103. [DOI]
- [4] Zayas, V. A., Low, S. S., Mahin, S. A. (1990): A Simple Pendulum Technique for Achieving Seismic Isolation, *Earthquake Spectra* 6, 317–334. [DOI]
- [5] Mokha, A., Constantinou, M. C., Reinhorn, A. M. (1990): Teflon Bearings in Seismic Base Isolation I: Testing, *Journal of Structural Engineering* 116, 438–454. [DOI]
- [6] Skinner, R. I., Kelly, J. M., Heine, A. J. (1975): Hysteretic Dampers for Earthquake Resistant Structures, *Earthquake Engineering and Structural Dynamics* 3, 287–296. [DOI]
- [7] Ene, D., Yamada, S., Jiao, Y., Kishiki, S., Konishi, Y. (2017): Reliability of U-shaped Steel Dampers Used in Base-Isolated Structures Subjected to Biaxial Excitation, *Earthquake Engineering & Structural Dynamics* 46, 621–639. [DOI]
- [8] Oh, S., Song, S., Lee, S., Kim, H. (2013): Experimental Study of Seismic Performance of Base-Isolated Frames with U-shaped Hysteretic Energy-Dissipating Devices, *Engineering Structures* 56, 2014–2027. [DOI]
- [9] Jiao, Y., Kishiki, S., Yamada, S., Ene, D., Konishi, Y., Hoashi, Y., Terashima, M. (2014): Low Cyclic Fatigue and Hysteretic Behavior of U-shaped Steel Dampers for Seismically Isolated Buildings under Dynamic Cyclic Loadings, *Earthquake Engineering Structural Dynamics* 44(10): 1523–1538. [DOI]
- [10] Jankowski, R., Seleemah, A., El-Khoribi, S., Elwardany, H. (2015): Experimental Study on Pounding between Structures During Damaging Earthquakes, *Key Engineering Materials* Vol. 627, 249–252. [DOI]
- [11] Serino, G., Occhiuzzi, A. (2003): A Semi-Active Oleodynamic Damper for Earthquake Control: Part 1: Design, Manufacturing and Experimental Analysis of the Device. *Bulletin of Earthquake Engineering* 1: 269–301. [DOI]

- [12] Tian, L., Fu, Z., Pan, H., Ma, R., Liu, Y. (2019): Experimental and Numerical Study on the Collapse Failure of Long-Span Transmission Tower-Line Systems Subjected to Extremely Severe Earthquakes, *Earthquakes and Structures* 16 No. 5. [DOI]
- [13] UNCRD (1995): Comprehensive Study of the Great Hanshin Earthquake, UNCRD Research Report Series No. 12, United Nations Centre for Regional Development (UNCRD), Nagoya, Japan.
- [14] Ghasemi, H., Cooper, J. D., Imbsen, R., Piskin, H., Inal, F., Tiras, A. (2000): The November 1999 Duzce Earthquake: Post- earthquake Investigation of the Structures on the TEM, Publication No. FHWA-RD-00-146, Federal Highway Administration Report.
- [15] Erdik, M. (2001): Report on 1999 Kocaeli and Duzce (Turkey) Earthquakes, *Structural Control for Civil and Infrastructure Engineering*, pp. 149-186 (2001). [DOI]
- [16] Ristic, J., Misini, M., Ristic, D., Guri, Z., Pllana, N. (2017): Seismic Upgrading of Isolated Bridges with SF-ED Devices: Shaking Table Tests of Large-Scale Model, *Gradjevinar*, 2147-2017. [DOI]
- [17] Ristic, J., Brujic, Z., Ristic, D., Folic, R., Boskovic, M. (2021): Upgrading of Isolated Bridges with Space-Bar Energy-Dissipation Devices: Shaking Table Test, *Advances in Structural Engineering*, June 23, 2021; pp. 2948–2965.
- [18] Ristic, J. (2016): Modern Technology for Seismic Protection of Bridge Structures Applying Advanced System for Modification of Earthquake Response, PhD Thesis, Institute of Earthquake Engineering and Engineering Seismology (IZIIS), “SS Cyril and Methodius” University, Skopje, Macedonia.
- [19] Candeias, P., Costa, A. C., Coelho, E. (2004): Shaking Table Tests of 1:3 Reduced Scale Models of Four-Story Unreinforced Masonry Buildings, 13th World Conference on Earthquake Engineering, Vancouver, Paper: 2199.
- [20] Ristic, D. (1988): Nonlinear Behavior and Stress-Strain Based Modeling of Reinforced Concrete Structures Under Earthquake Induced Bending and Varying Axial Loads, Doctoral Dissertation, School of Civil Engineering, Kyoto University, Japan.
- [21] Ristic, D., Ristic J. (2012): Advanced Integrated 2G3 Response Modification Method for Seismic Upgrading of New and Existing Bridges, 15th World Conf. on Earthquake Engineering, (WCEE), Lisbon.
- [22] Ristic, J., Ristic D., Behrami, R., Hristovski, V., (2024): Adaptive Seismic Upgrading of Isolated Bridges with C-Gapped Devices: Model Testing, *Civil Engineering Journal*, Vol. 10, No. 09, September, 2024.
- [23] Ristic, J., Veseli V., Misini, L., Ristic, D., (2023): Seismic protection of masonry and infilled frame buildings using upgraded sliding isolation system with SF devices, *Proceedings of the 2<sup>nd</sup> Croatian Conference on Earthquake Engineering - 2CroCEE*, Zagreb, Croatia - March 22 to 24, 2023.